Geometry and Computation

Yakov Berchenko-Kogan

Pennsylvania State University

Geometry and Computation

1. Olfactory space (mathematical neuroscience).
2. Three numerical analysis vignettes.
3. Mean curvature flow.

Part 1

Olfactory space

What is the space of odors?

Vision analogy

Figure: Nearby visual stimuli (left) and the configuration space (right)

What is the space of odors?

Vision analogy

Figure: Nearby visual stimuli (left) and the configuration space (right)

When are odors "nearby"?

What is the space of odors?

Vision analogy

Figure: Nearby visual stimuli (left) and the configuration space (right)

When are odors "nearby"?

- Ask the neurons!

What is the space of odors?

Vision analogy

Figure: Nearby visual stimuli (left) and the configuration space (right)

When are odors “nearby”?

- Ask the neurons!
- Experimental data: matrix r_{ia} of response of sensory neuron of type i to odorant a.

What is the space of odors?

Vision analogy

Figure: Nearby visual stimuli (left) and the configuration space (right)

When are odors "nearby"?

- Ask the neurons!
- Experimental data: matrix r_{ia} of response of sensory neuron of type i to odorant a.
- Goal: develop a configuration space where each odorant a corresponds to a point x_a, so that nearby odorants elicit similar responses.

Olfactory model

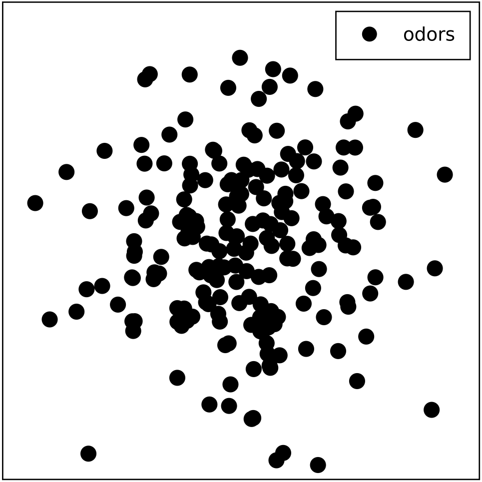

Configuration space (olfactory space)

Olfactory model

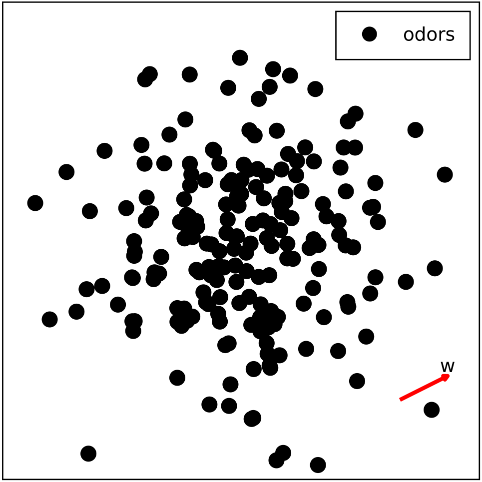

Configuration space (olfactory space)

Olfactory model

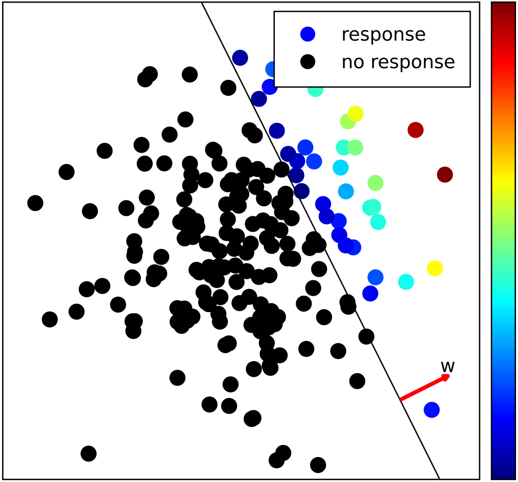

Configuration space (olfactory space)

Olfactory model

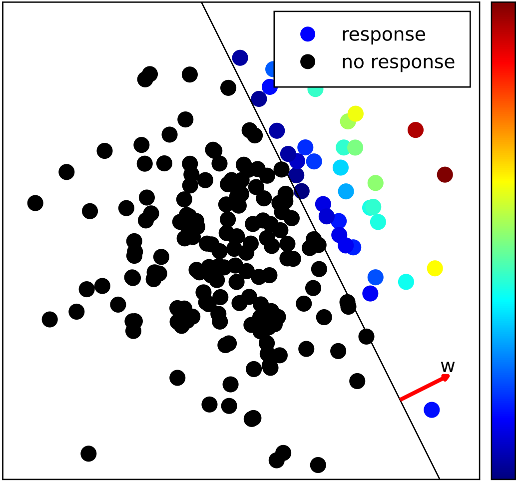

Configuration space (olfactory space)

$$r = f(w \cdot x)$$

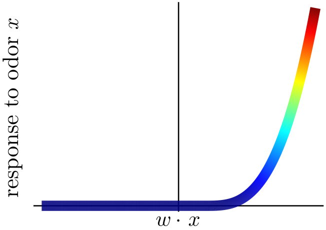

f is an unknown monotone function.

Finding olfactory space

Model

- Each odorant a has an associated point $x_a \in \mathbb{R}^d$.
- The neurons with olfactory receptor i have an associated vector $w_i \in \mathbb{R}^d$ and monotone increasing function f_i.
- The response of neurons i to odorant a is given by

$$r_{ia} = f_i(w_i \cdot x_a).$$

Goal

- Given responses r_{ia}, find (approximately) f_i, $w_i \in \mathbb{R}^d$, and $x_a \in \mathbb{R}^d$, with d not too large.
- The points x_a form olfactory space, a space whose points are odors.

Challenge: nonlinearity

Original problem

Given responses r_{ia}, find f_i, $w_i \in \mathbb{R}^d$, and $x_a \in \mathbb{R}^d$, with d not too large, such that

$$r_{ia} \approx f_i(w_i \cdot x_a).$$

Challenge: nonlinearity

Original problem

Given responses r_{ia}, find f_i, $w_i \in \mathbb{R}^d$, and $x_a \in \mathbb{R}^d$, with d not too large, such that

$$r_{ia} \approx f_i(w_i \cdot x_a).$$

An easier, linear, problem

Challenge: nonlinearity

Original problem

Given responses r_{ia}, find f_i, $w_i \in \mathbb{R}^d$, and $x_a \in \mathbb{R}^d$, with d not too large, such that

$$r_{ia} \approx f_i(w_i \cdot x_a).$$

An easier, linear, problem

- Given p_{ia} find $w_i \in \mathbb{R}^d$, and $x_a \in \mathbb{R}^d$, with d not too large, such that

$$p_{ia} \approx w_i \cdot x_a$$

Challenge: nonlinearity

Original problem

Given responses r_{ia}, find f_i, $w_i \in \mathbb{R}^d$, and $x_a \in \mathbb{R}^d$, with d not too large, such that

$$r_{ia} \approx f_i(w_i \cdot x_a).$$

An easier, linear, problem

- Given p_{ia} find $w_i \in \mathbb{R}^d$, and $x_a \in \mathbb{R}^d$, with d not too large, such that

$$p_{ia} \approx w_i \cdot x_a$$

- Equivalently, given $m \times n$ matrix P, find $m \times d$ matrix W and $d \times n$ matrix X such that

$$P \approx WX.$$

Challenge: nonlinearity

Original problem

Given responses r_{ia}, find f_i, $w_i \in \mathbb{R}^d$, and $x_a \in \mathbb{R}^d$, with d not too large, such that

$$r_{ia} \approx f_i(w_i \cdot x_a).$$

An easier, linear, problem

- Given p_{ia} find $w_i \in \mathbb{R}^d$, and $x_a \in \mathbb{R}^d$, with d not too large, such that

$$p_{ia} \approx w_i \cdot x_a$$

- Equivalently, given $m \times n$ matrix P, find $m \times d$ matrix W and $d \times n$ matrix X such that

$$P \approx WX.$$

- Solution: singular value decomposition of P (principal component analysis).

Addressing nonlinearity (joint with V. Itskov)

Original problem

Given responses r_{ia}, find f_i, $w_i \in \mathbb{R}^d$, and $x_a \in \mathbb{R}^d$, with d not too large, such that

$$r_{ia} \approx f_i(w_i \cdot x_a).$$

Outline of method

Addressing nonlinearity (joint with V. Itskov)

Original problem

Given responses r_{ia}, find f_i, $w_i \in \mathbb{R}^d$, and $x_a \in \mathbb{R}^d$, with d not too large, such that

$$r_{ia} \approx f_i(w_i \cdot x_a).$$

Outline of method

- With assumptions on the probability distribution of the x_a, for each i we can get the distribution of $w_i \cdot x_a$. Comparing with r_{ia}, we can estimate f_i.

Addressing nonlinearity (joint with V. Itskov)

Original problem

Given responses r_{ia}, find f_i, $w_i \in \mathbb{R}^d$, and $x_a \in \mathbb{R}^d$, with d not too large, such that

$$r_{ia} \approx f_i(w_i \cdot x_a).$$

Outline of method

- With assumptions on the probability distribution of the x_a, for each i we can get the distribution of $w_i \cdot x_a$. Comparing with r_{ia}, we can estimate f_i.

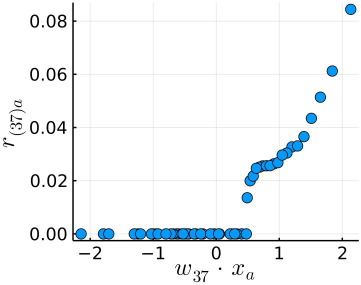

Addressing nonlinearity (joint with V. Itskov)

Original problem

Given responses r_{ia}, find f_i, $w_i \in \mathbb{R}^d$, and $x_a \in \mathbb{R}^d$, with d not too large, such that

$$r_{ia} \approx f_i(w_i \cdot x_a).$$

Outline of method

- With assumptions on the probability distribution of the x_a, for each i we can get the distribution of $w_i \cdot x_a$. Comparing with r_{ia}, we can estimate f_i.
- Reduce to linear problem:

$$f_i^{-1}(r_{ia}) \approx w_i \cdot x_a.$$

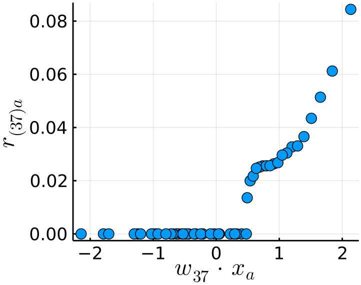

Olfactory space: odorant concentration

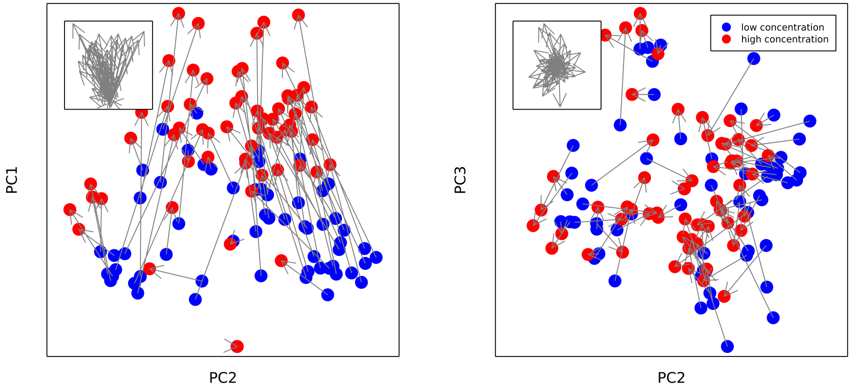

Figure: Olfactory space. Joint work with V. Itskov. Data from M. Wachowiak.

Olfactory space: odorant chemical class

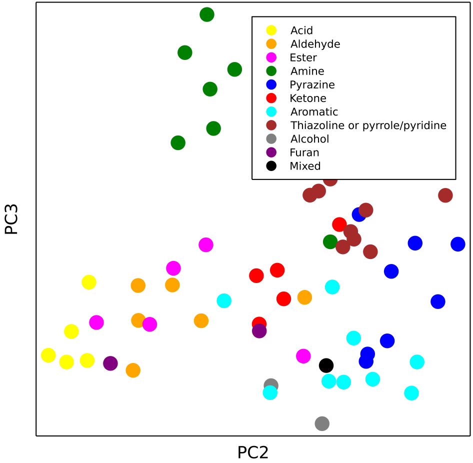

Figure: Olfactory space. Joint work with V. Itskov. Data from M. Wachowiak.

Part 2

Geometry and numerical analysis: three vignettes

Vignette 1

Numerical methods that respect conservation laws for Maxwell's equations and the Yang–Mills equations

Toy example illustrating conservation law failure

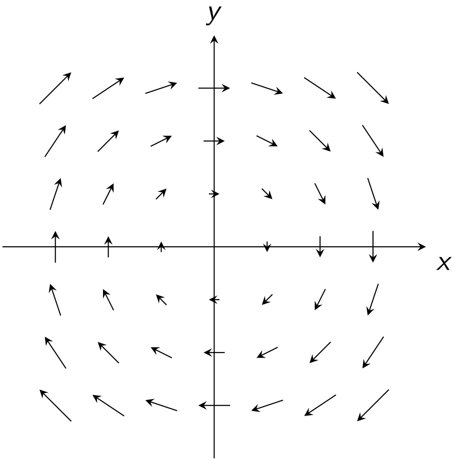

Figure: Phase space diagram for the harmonic oscillator, $\dot{x} = y, \dot{y} = -x$.

Toy example illustrating conservation law failure

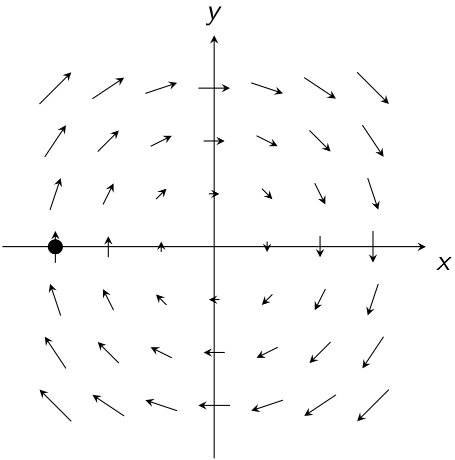

Figure: Phase space diagram for the harmonic oscillator, $\dot{x} = y, \dot{y} = -x$.

Toy example illustrating conservation law failure

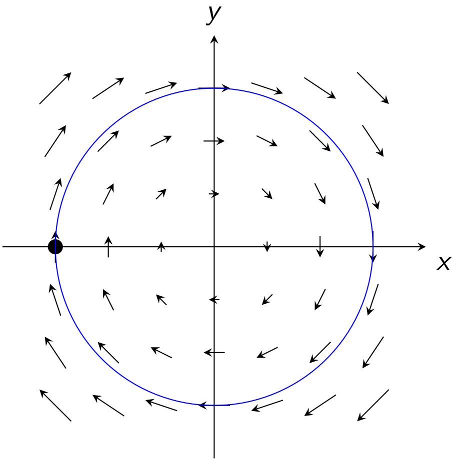

Figure: Phase space diagram for the harmonic oscillator, $\dot{x} = y, \dot{y} = -x$.

Toy example illustrating conservation law failure

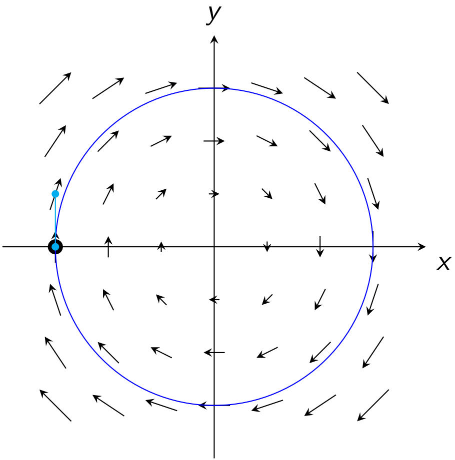

Figure: Phase space diagram for the harmonic oscillator, $\dot{x} = y, \dot{y} = -x$.

Toy example illustrating conservation law failure

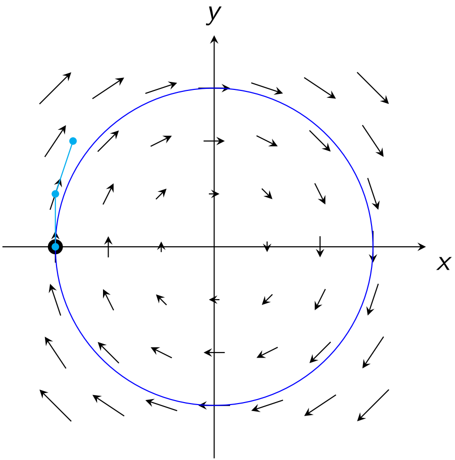

Figure: Phase space diagram for the harmonic oscillator, $\dot{x} = y, \dot{y} = -x$.

Toy example illustrating conservation law failure

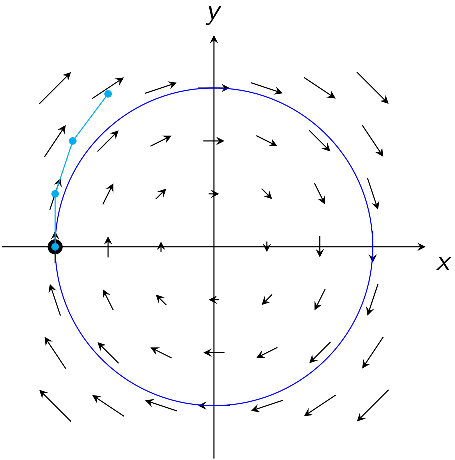

Figure: Phase space diagram for the harmonic oscillator, $\dot{x} = y, \dot{y} = -x$.

Toy example illustrating conservation law failure

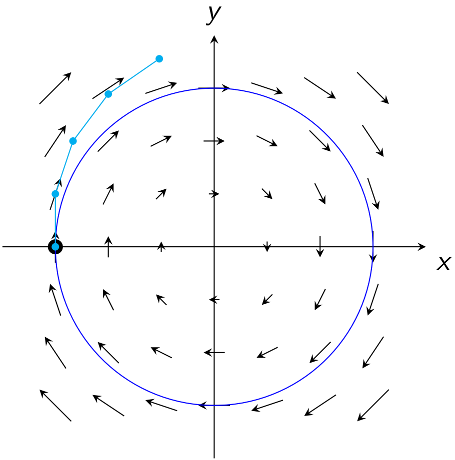

Figure: Phase space diagram for the harmonic oscillator, $\dot{x} = y, \dot{y} = -x$.

Toy example illustrating conservation law failure

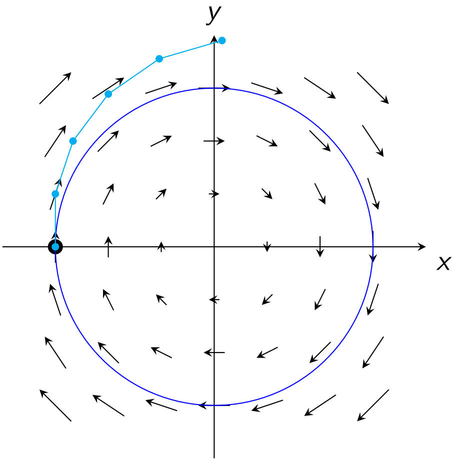

Figure: Phase space diagram for the harmonic oscillator, $\dot{x} = y, \dot{y} = -x$.

Toy example illustrating conservation law failure

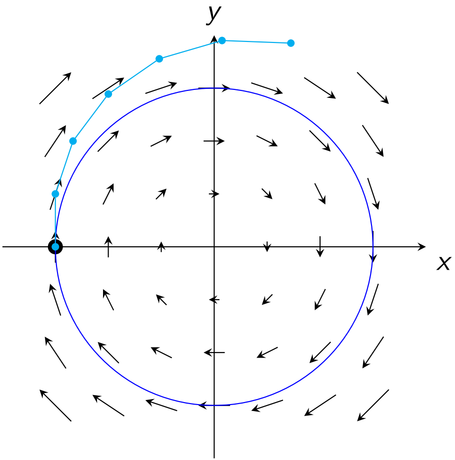

Figure: Phase space diagram for the harmonic oscillator, $\dot{x} = y, \dot{y} = -x$.

Toy example illustrating conservation law failure

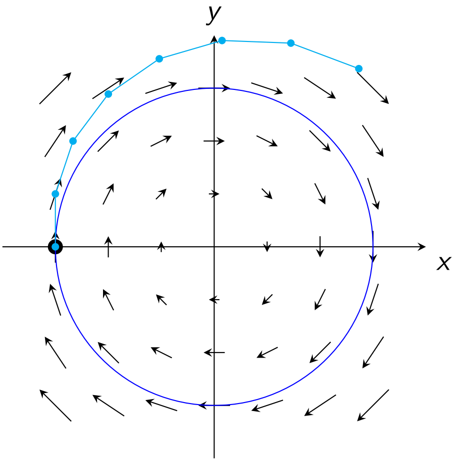

Figure: Phase space diagram for the harmonic oscillator, $\dot{x} = y, \dot{y} = -x$.

Toy example illustrating conservation law failure

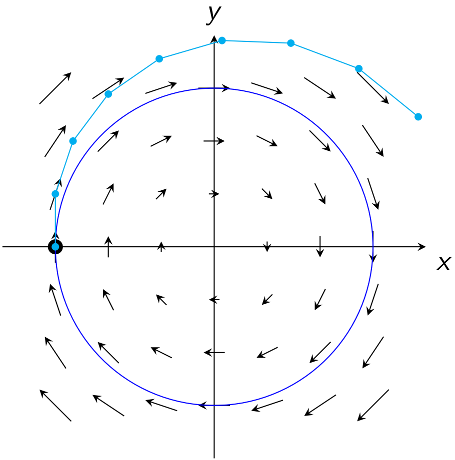

Figure: Phase space diagram for the harmonic oscillator, $\dot{x} = y, \dot{y} = -x$.

Toy example illustrating conservation law failure

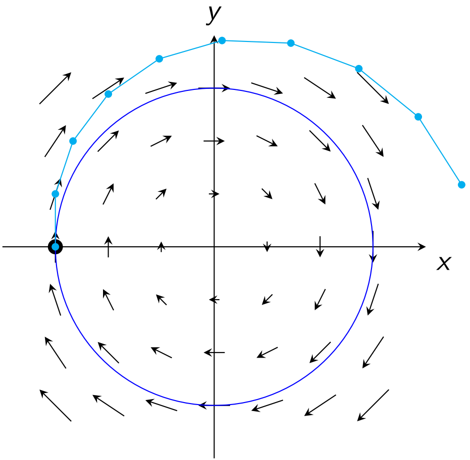

Figure: Phase space diagram for the harmonic oscillator, $\dot{x} = y, \dot{y} = -x$.

Toy example illustrating conservation law failure

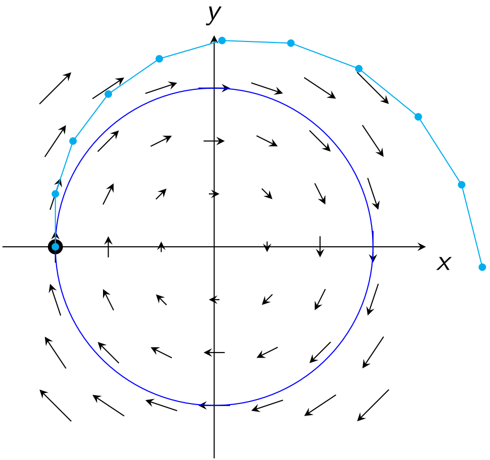

Figure: Phase space diagram for the harmonic oscillator, $\dot{x} = y, \dot{y} = -x$.

Toy example illustrating conservation law failure

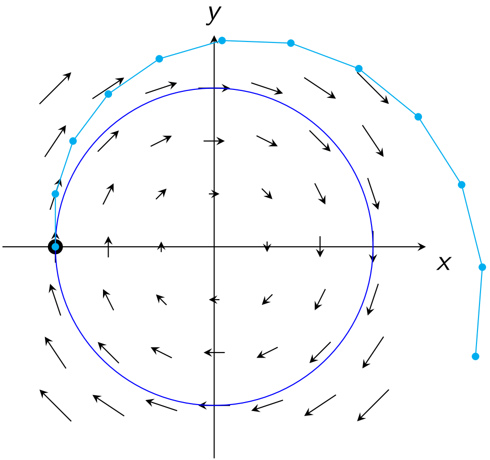

Figure: Phase space diagram for the harmonic oscillator, $\dot{x} = y, \dot{y} = -x$.

Toy example illustrating conservation law failure

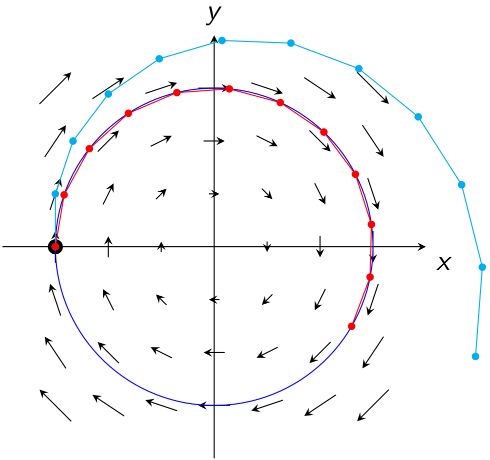

Figure: Phase space diagram for the harmonic oscillator, $\dot{x} = y, \dot{y} = -x$.

Charge conservation

- Maxwell's equations of electromagnetism have charge conservation.

Charge conservation

- Maxwell's equations of electromagnetism have charge conservation.
- The Yang-Mills equations are a nonlinear generalization of Maxwell's equations.

Charge conservation

- Maxwell's equations of electromagnetism have charge conservation.
- The Yang-Mills equations are a nonlinear generalization of Maxwell's equations.

Y. I. Berchenko-Kogan and A. Stern.
Constraint-preserving hybrid finite element methods for Maxwell's equations.
Found. Comput. Math., 2021.

Charge conservation

- Maxwell's equations of electromagnetism have charge conservation.
- The Yang-Mills equations are a nonlinear generalization of Maxwell's equations.

Y. I. Berchenko-Kogan and A. Stern.
Constraint-preserving hybrid finite element methods for Maxwell's equations.
Found. Comput. Math., 2021.

Y. I. Berchenko-Kogan and A. Stern.
Charge-conserving hybrid methods for the Yang–Mills equations.
SMAI J. Comput. Math., 2021.

Vignette 2

Finite element exterior calculus

Discrete scalar functions

How to represent a discrete function?

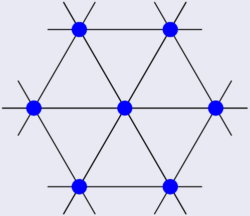

Discrete scalar functions

How to represent a discrete function?

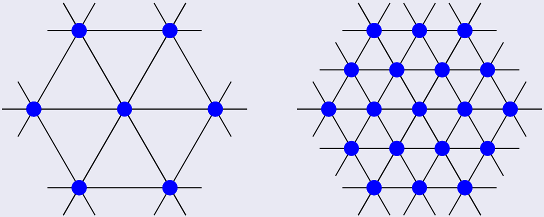

Discrete scalar functions

How to represent a discrete function?

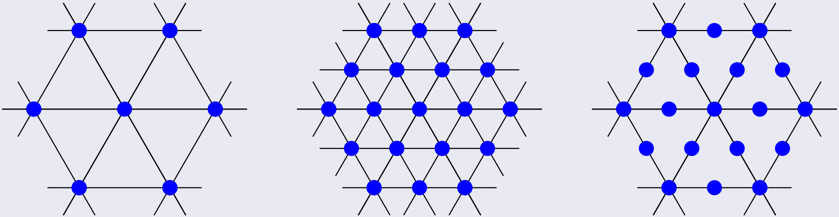

Figure: Piecewise linear on a finer mesh, or piecewise quadratic?

Discrete scalar functions

How to represent a discrete function?

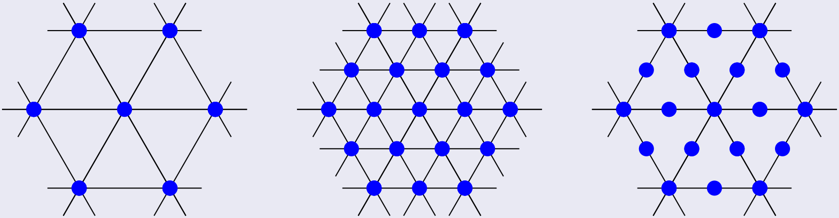

Figure: Piecewise linear on a finer mesh, or piecewise quadratic?

Why use higher degree?

- Using piecewise quadratics gives us faster convergence.
  - cf. trapezoid rule (linear) vs. Simpson's rule (quadratic).
- Sometimes there is no convergence at all unless we use higher degree.
  - e.g. mean curvature flow (Kovács, Li, Lubich, 2019).

Vector fields

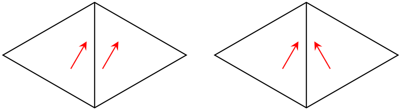

Figure: Full continuity (left) vs. tangential continuity (right)

Why impose tangential continuity rather than full continuity?

Vector fields

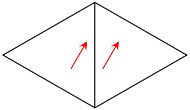

Figure: Full continuity (left) vs. tangential continuity (right)

Why impose tangential continuity rather than full continuity?

- The gradient of a piecewise polynomial scalar function has only tangential continuity.

Vector fields

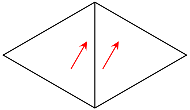

Figure: Full continuity (left) vs. tangential continuity (right)

Why impose tangential continuity rather than full continuity?

- The gradient of a piecewise polynomial scalar function has only tangential continuity.
- Tangential continuity is the minimum needed for line integrals to be well-defined.

Vector fields

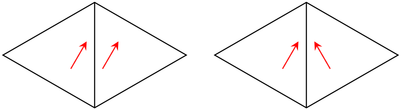

Figure: Full continuity (left) vs. tangential continuity (right)

Why impose tangential continuity rather than full continuity?

- The gradient of a piecewise polynomial scalar function has only tangential continuity.
- Tangential continuity is the minimum needed for line integrals to be well-defined.
- Imposing "unnatural" continuity can lead to wrong answers.

Vector fields

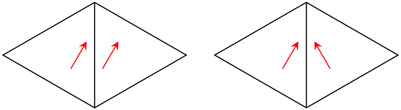

Figure: Full continuity (left) vs. tangential continuity (right)

Why impose tangential continuity rather than full continuity?

- The gradient of a piecewise polynomial scalar function has only tangential continuity.
- Tangential continuity is the minimum needed for line integrals to be well-defined.
- Imposing "unnatural" continuity can lead to wrong answers.

- What are the degrees of freedom for vector fields with tangential continuity?

Periodic Table of the Finite Elements

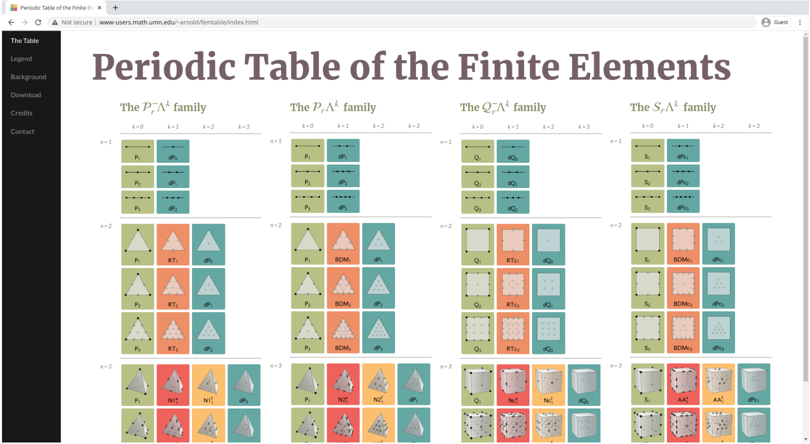

Figure: Arnold and Logg, 2014

Periodic Table of the Finite Elements

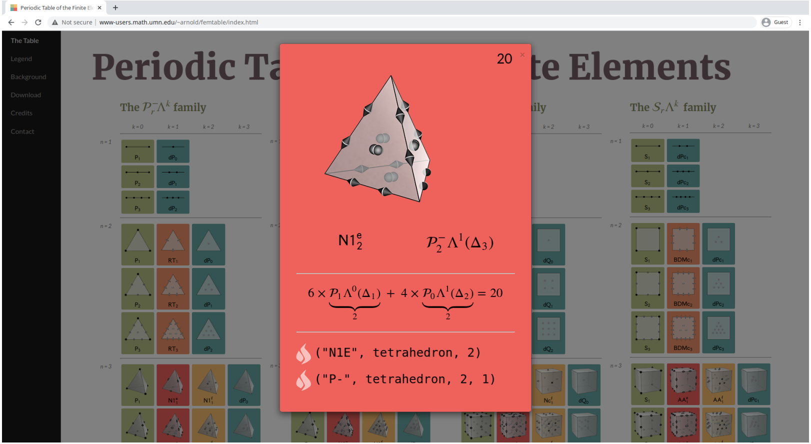

Figure: Arnold and Logg, 2014

References

Y. I. Berchenko-Kogan.
Duality in finite element exterior calculus and Hodge duality on the sphere.
Found. Comput. Math., 2021.

Y. I. Berchenko-Kogan.
Symmetric bases for finite element exterior calculus spaces.
https://arxiv.org/abs/2112.06065.

Vignette 3

Finite element differential geometry

Discrete manifolds

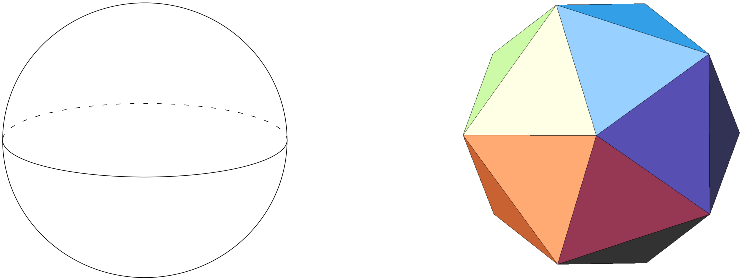

Figure: Image credit (right): Wikipedia

Discrete manifolds

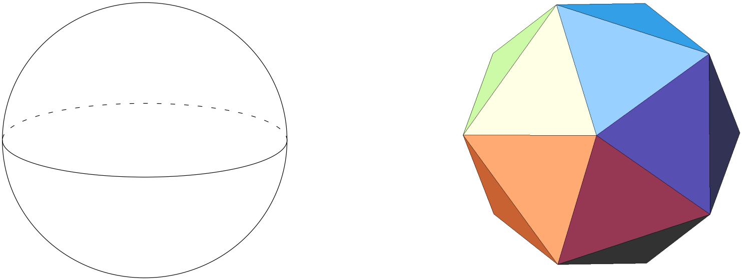

Figure: Image credit (right): Wikipedia

Discrete differential geometry

- Scalar functions, vector fields, line integrals, curvature, differential forms, Levi–Civita connection, Laplacian, ...

From discrete to finite element

Higher order objects

From discrete to finite element

Higher order objects

- Scalar functions, vector fields, differential forms (Arnold, Falk, Winther, 2006).

From discrete to finite element

Higher order objects

- Scalar functions, vector fields, differential forms (Arnold, Falk, Winther, 2006).
- Riemannian metric (Li, 2018).

From discrete to finite element

Higher order objects

- Scalar functions, vector fields, differential forms (Arnold, Falk, Winther, 2006).
- Riemannian metric (Li, 2018).
- Levi–Civita connection, curvature?

From discrete to finite element

Higher order objects

- Scalar functions, vector fields, differential forms (Arnold, Falk, Winther, 2006).
- Riemannian metric (Li, 2018).
- Levi–Civita connection, curvature?

Y. I. Berchenko-Kogan and E. Gawlik.
Finite element approximation of the Levi–Civita connection and its curvature in two dimensions.
https://arxiv.org/abs/2111.02512.

From discrete to finite element

Higher order objects

- Scalar functions, vector fields, differential forms (Arnold, Falk, Winther, 2006).
- Riemannian metric (Li, 2018).
- Levi–Civita connection, curvature?

Y. I. Berchenko-Kogan and E. Gawlik.
Finite element approximation of the Levi–Civita connection and its curvature in two dimensions.
https://arxiv.org/abs/2111.02512.

Y. I. Berchenko-Kogan and E. Gawlik.
Discrete connections on deforming triangulations.
In preparation.

Part 3

Mean curvature flow

Curve shortening flow

$$\frac{d}{dt}\mathbf{x} = -\kappa(\mathbf{x})\mathbf{n}.$$

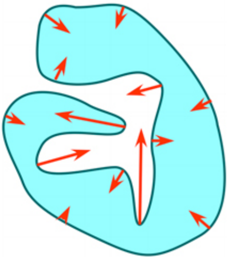

Figure: Curve shortening flow. Image credit: Treibergs. Video credit: Angenent.

Mean curvature flow

$$\frac{d}{dt}\mathbf{x} = -H(\mathbf{x})\mathbf{n}$$

Figure: Mean curvature flow. Video credit: Kovács.

Mean curvature flow singularities

- Categorize singularities by zooming in at the singular point just before the singular time.

Mean curvature flow singularities

- Categorize singularities by zooming in at the singular point just before the singular time.
  - round sphere

Mean curvature flow singularities

- Categorize singularities by zooming in at the singular point just before the singular time.
  - round sphere
  - round cylinder

Mean curvature flow singularities

- Categorize singularities by zooming in at the singular point just before the singular time.
    - round sphere
    - round cylinder
    - others?

Mean curvature flow singularities

- Categorize singularities by zooming in at the singular point just before the singular time.
  - round sphere
  - round cylinder
  - others?
- Such a limiting surface must be a self-shrinker.

Mean curvature flow singularities

- Categorize singularities by zooming in at the singular point just before the singular time.
  - round sphere
  - round cylinder
  - others?
- Such a limiting surface must be a self-shrinker.
  - A self-shrinker is a surface that evolves under mean curvature flow by dilations.

Mean curvature flow singularities

- Categorize singularities by zooming in at the singular point just before the singular time.
    - round sphere
    - round cylinder
    - others?
- Such a limiting surface must be a self-shrinker.
    - A self-shrinker is a surface that evolves under mean curvature flow by dilations.
- Are there other self-shrinkers?

Mean curvature flow singularities

- Categorize singularities by zooming in at the singular point just before the singular time.
  - round sphere
  - round cylinder
  - others?
- Such a limiting surface must be a self-shrinker.
  - A self-shrinker is a surface that evolves under mean curvature flow by dilations.
- Are there other self-shrinkers?
  - Yes, a torus (Angenent, 1989).

Mean curvature flow singularities

- Categorize singularities by zooming in at the singular point just before the singular time.
  - round sphere
  - round cylinder
  - others?
- Such a limiting surface must be a self-shrinker.
  - A self-shrinker is a surface that evolves under mean curvature flow by dilations.
- Are there other self-shrinkers?
  - Yes, a torus (Angenent, 1989).
  - Many others (Kapouleas, Kleene, Møller, 2011).

The Angenent torus

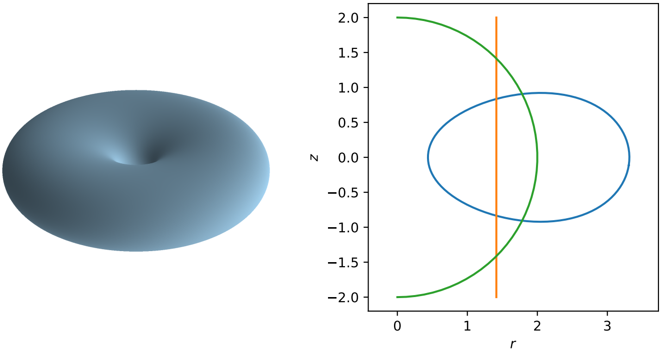

Figure: The Angenent torus (left) and its cross-section (right), with the self-shrinking sphere (green) and cylinder (orange) for comparison.

Angenent torus intuition

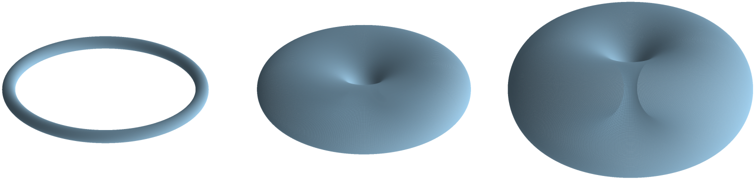

Figure: Meridian collapse (left), inner longitude collapse (right), just right (middle).

Stability of self-shrinkers

- For curve shortening flow, if we perturb a circle, the curve will return to a circular shape as it shrinks.

Stability of self-shrinkers

- For curve shortening flow, if we perturb a circle, the curve will return to a circular shape as it shrinks.
- If we perturb a round sphere a little, it will also return to being round as it shrinks.

Stability of self-shrinkers

- For curve shortening flow, if we perturb a circle, the curve will return to a circular shape as it shrinks.
- If we perturb a round sphere a little, it will also return to being round as it shrinks.
- The Angenent torus might not.

Stability of self-shrinkers

- For curve shortening flow, if we perturb a circle, the curve will return to a circular shape as it shrinks.
- If we perturb a round sphere a little, it will also return to being round as it shrinks.
- The Angenent torus might not.
  - e.g. perturbations could cause the meridian to collapse too soon.

Stability of self-shrinkers

- For curve shortening flow, if we perturb a circle, the curve will return to a circular shape as it shrinks.
- If we perturb a round sphere a little, it will also return to being round as it shrinks.
- The Angenent torus might not.
  - e.g. perturbations could cause the meridian to collapse too soon.
- How unstable is it?

Critical points, stability, index

 

Figure: Stable critical point (left), unstable critical points (right)

Critical points, stability, index

Figure: Stable critical point (left), unstable critical points (right)

Morse index

Critical points, stability, index


Figure: Stable critical point (left), unstable critical points (right)

Morse index

- The index is the number of negative eigenvalues of the Hessian.

Critical points, stability, index

 

Figure: Stable critical point (left), unstable critical points (right)

Morse index

- The index is the number of negative eigenvalues of the Hessian.
- The corresponding eigenvectors give unstable “downward” directions.

Toy example illustrating critical curves and stability

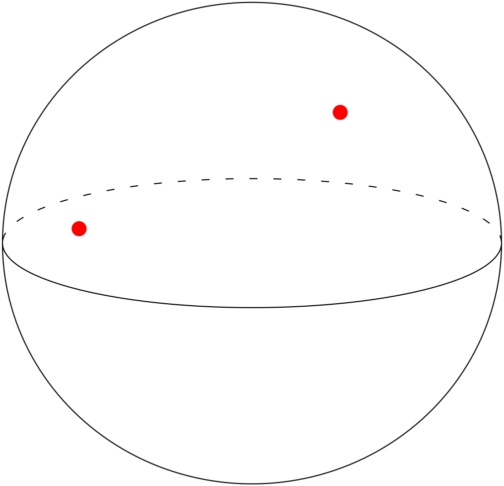

Figure: Geodesics are critical points of the length functional. Two cities can be connected with a stable geodesic and with an unstable geodesic.

Toy example illustrating critical curves and stability

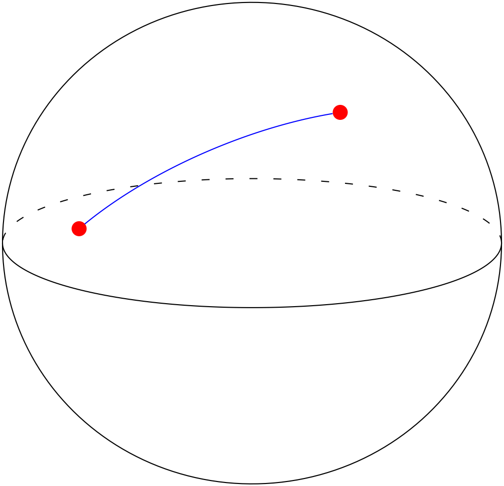

Figure: Geodesics are critical points of the length functional. Two cities can be connected with a stable geodesic and with an unstable geodesic.

Toy example illustrating critical curves and stability

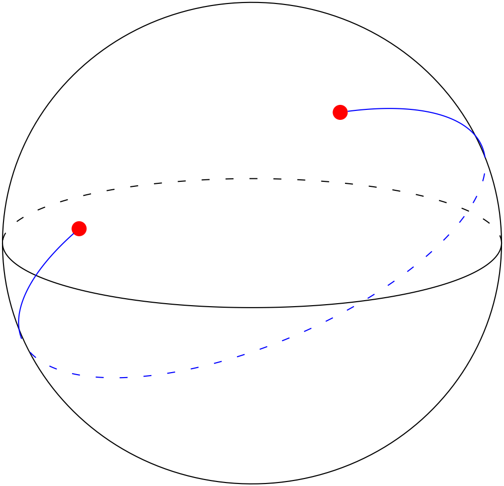

Figure: Geodesics are critical points of the length functional. Two cities can be connected with a stable geodesic and with an unstable geodesic.

Toy example illustrating index

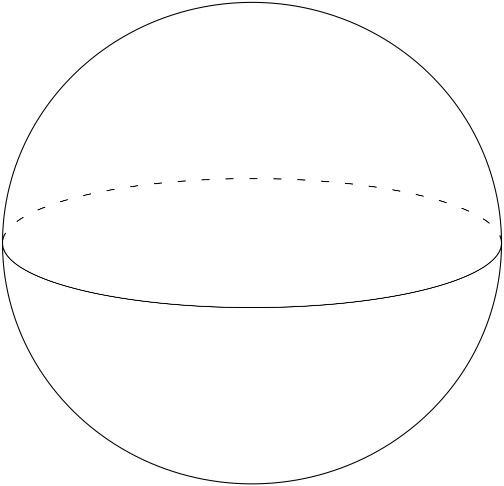

Figure: Stable and unstable variations of the equator.

Toy example illustrating index

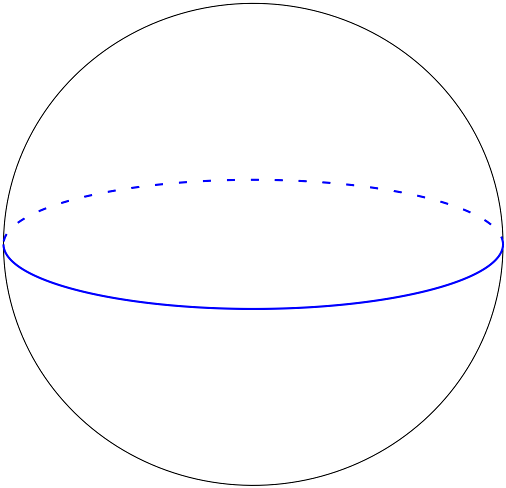

Figure: Stable and unstable variations of the equator.

Toy example illustrating index

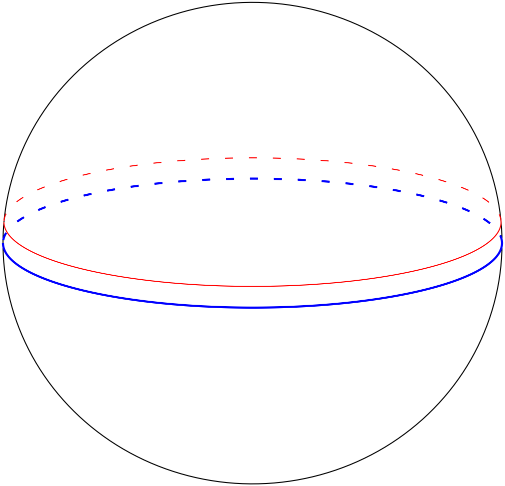

Figure: Stable and unstable variations of the equator.

Toy example illustrating index

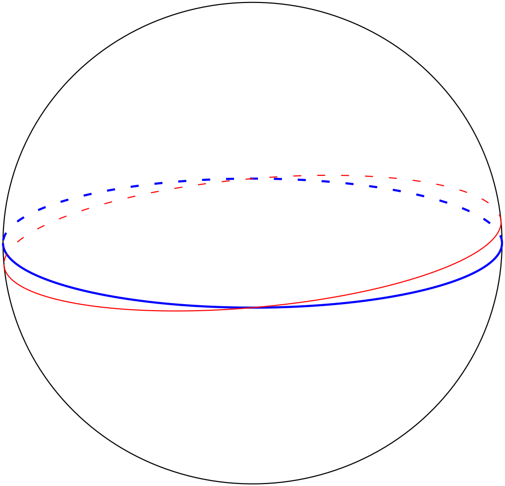

Figure: Stable and unstable variations of the equator.

Toy example illustrating index

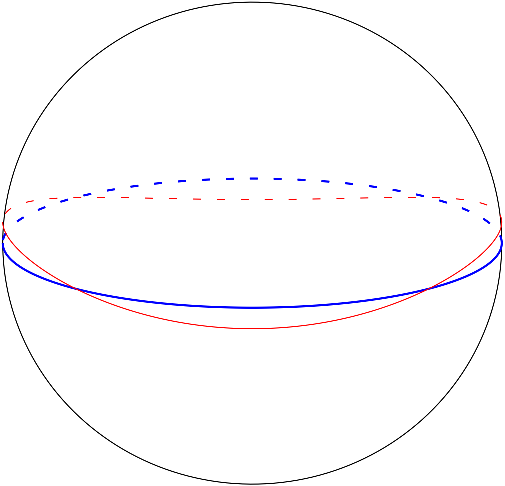

Figure: Stable and unstable variations of the equator.

Toy example illustrating index

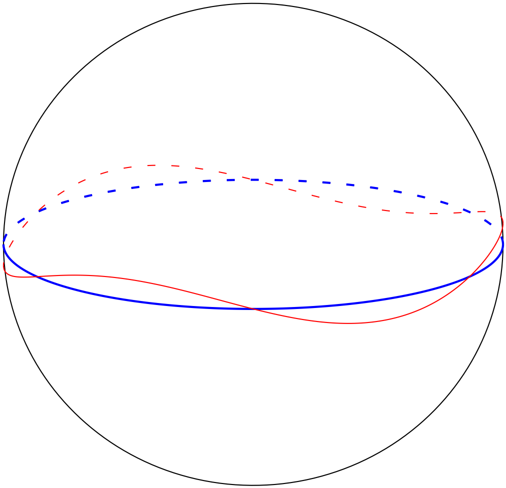

Figure: Stable and unstable variations of the equator.

A variational formulation for self-shrinkers

Theorem (Huisken, 1990)

A hypersurface $\Sigma \subset \mathbb{R}^{n+1}$ is a self-shrinker that becomes extinct at the origin after one unit of time if and only if it is a critical point of the weighted area functional called the F-functional.

$$F(\Sigma) = (4\pi)^{-n/2} \int_\Sigma e^{-|x|^2/4} \, dArea.$$

A variational formulation for self-shrinkers

Theorem (Huisken, 1990)

A hypersurface $\Sigma \subset \mathbb{R}^{n+1}$ is a self-shrinker that becomes extinct at the origin after one unit of time if and only if it is a critical point of the weighted area functional called the F-functional.

$$F(\Sigma) = (4\pi)^{-n/2} \int_{\Sigma} e^{-|x|^2/4} \, dArea.$$

i.e. for any family of surfaces Σ_s parametrized by s with $\Sigma_0 = \Sigma$, we have

$$\left.\frac{d}{ds}\right|_{s=0} F(\Sigma_s) = 0.$$

A variational formulation for self-shrinkers

Theorem (Huisken, 1990)

A hypersurface $\Sigma \subset \mathbb{R}^{n+1}$ is a self-shrinker that becomes extinct at the origin after one unit of time if and only if it is a critical point of the weighted area functional called the F-functional.

$$F(\Sigma) = (4\pi)^{-n/2} \int_\Sigma e^{-|x|^2/4}\, dArea.$$

i.e. for any family of surfaces Σ_s parametrized by s with $\Sigma_0 = \Sigma$, we have

$$\left.\frac{d}{ds}\right|_{s=0} F(\Sigma_s) = 0.$$

Morse index of a self-shrinker

- The index is the number of negative eigenvalues of the "Hessian".
- The corresponding eigenfunctions give variations that are unstable (decrease F).

The index of the Angenent torus

Index

The index of the Angenent torus

Index

- Count the number of negative eigenvalues of the Hessian (unstable variations, "downhill" directions).

The index of the Angenent torus

Index

- Count the number of negative eigenvalues of the Hessian (unstable variations, “downhill” directions).

Previously known unstable variations

The index of the Angenent torus

Index

- Count the number of negative eigenvalues of the Hessian (unstable variations, "downhill" directions).

Previously known unstable variations

- "Trivial" variations: dilation ($\lambda = -1$), three translations ($\lambda = -\frac{1}{2}$).

The index of the Angenent torus

Index

- Count the number of negative eigenvalues of the Hessian (unstable variations, “downhill” directions).

Previously known unstable variations

- “Trivial” variations: dilation ($\lambda = -1$), three translations ($\lambda = -\frac{1}{2}$).
- At least three other variations exist (Liu, 2016).

The index of the Angenent torus

Index

- Count the number of negative eigenvalues of the Hessian (unstable variations, “downhill” directions).

Previously known unstable variations

- “Trivial” variations: dilation ($\lambda = -1$), three translations ($\lambda = -\frac{1}{2}$).
- At least three other variations exist (Liu, 2016).

Numerically computing the index

The index of the Angenent torus

Index

- Count the number of negative eigenvalues of the Hessian (unstable variations, “downhill” directions).

Previously known unstable variations

- “Trivial” variations: dilation ($\lambda = -1$), three translations ($\lambda = -\frac{1}{2}$).
- At least three other variations exist (Liu, 2016).

Numerically computing the index

- Once we discretize, the F-functional is a functional on a (large) finite-dimensional space of discrete surfaces.

The index of the Angenent torus

Index

- Count the number of negative eigenvalues of the Hessian (unstable variations, "downhill" directions).

Previously known unstable variations

- "Trivial" variations: dilation ($\lambda = -1$), three translations ($\lambda = -\frac{1}{2}$).
- At least three other variations exist (Liu, 2016).

Numerically computing the index

- Once we discretize, the F-functional is a functional on a (large) finite-dimensional space of discrete surfaces.
- At a critical point ($\nabla F = 0$), we compute the Hessian matrix $\nabla^2 F$.

The index of the Angenent torus

Index

- Count the number of negative eigenvalues of the Hessian (unstable variations, “downhill” directions).

Previously known unstable variations

- “Trivial” variations: dilation ($\lambda = -1$), three translations ($\lambda = -\frac{1}{2}$).
- At least three other variations exist (Liu, 2016).

Numerically computing the index

- Once we discretize, the F-functional is a functional on a (large) finite-dimensional space of discrete surfaces.
- At a critical point ($\nabla F = 0$), we compute the Hessian matrix $\nabla^2 F$.
- The index is the number of negative eigenvalues of this matrix.

The index of the Angenent torus

Index

- Count the number of negative eigenvalues of the Hessian (unstable variations, "downhill" directions).

Previously known unstable variations

- "Trivial" variations: dilation ($\lambda = -1$), three translations ($\lambda = -\frac{1}{2}$).
- At least three other variations exist (Liu, 2016).

Numerically computing the index

- Once we discretize, the F-functional is a functional on a (large) finite-dimensional space of discrete surfaces.
- At a critical point ($\nabla F = 0$), we compute the Hessian matrix $\nabla^2 F$.
- The index is the number of negative eigenvalues of this matrix.
- The corresponding eigenfunctions are the unstable variations.

Index results (YBK, 2020)

$k = 0$	$k = 1$	$k = 2$
$\lambda_0 \approx -3.740$	$\lambda_0 = -1$	$\lambda_0 \approx -0.488$
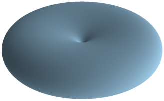	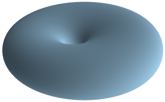	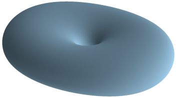
$\lambda_1 = -1$	$\lambda_0 = -1$	$\lambda_0 \approx -0.488$
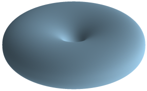	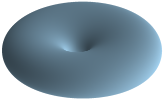	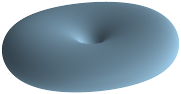
$\lambda_2 = -\frac{1}{2}$	$\lambda_1 = -\frac{1}{2}$	
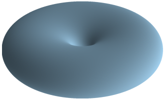	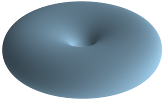	
	$\lambda_1 = -\frac{1}{2}$	
	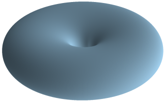	

References

Yakov Berchenko-Kogan.
The entropy of the Angenent torus is approximately 1.85122.
Experimental Math., 2019.

Yakov Berchenko-Kogan.
Bounds on the index of rotationally symmetric self-shrinking tori.
Geom. Dedicata, 2021.

Yakov Berchenko-Kogan.
Numerically computing the index of mean curvature flow self-shrinkers.
Results Math., 2022.

Future directions

- Higher-dimensional Angenent doughnuts $S^1 \times S^{n-1} \subset \mathbb{R}^{n+1}$.
- Other self-shrinkers determined by a 1D cross-section.
- General self-shrinking surfaces (without symmetry).
- Error bounds.

Thank you

The entropy of self-shrinkers

The critical value of the F-functional, called the entropy of the self-shrinker, is helpful in understanding what kinds of singularities can occur.

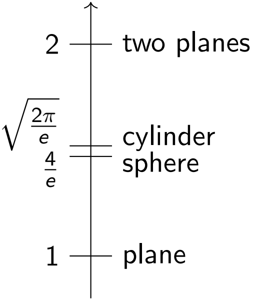

Figure: Entropies of self-shrinking surfaces

The entropy of self-shrinkers

The critical value of the F-functional, called the entropy of the self-shrinker, is helpful in understanding what kinds of singularities can occur.

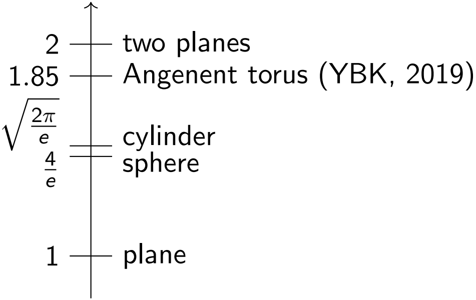

Figure: Entropies of self-shrinking surfaces

The entropy of self-shrinkers

The critical value of the F-functional, called the entropy of the self-shrinker, is helpful in understanding what kinds of singularities can occur.

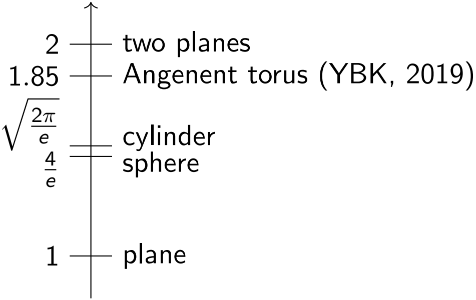

Figure: Entropies of self-shrinking surfaces

Earlier work (Drugan and Nguyen, 2018): the entropy of the Angenent torus is less than 2.

Numerical estimates of the entropy of the Angenent torus

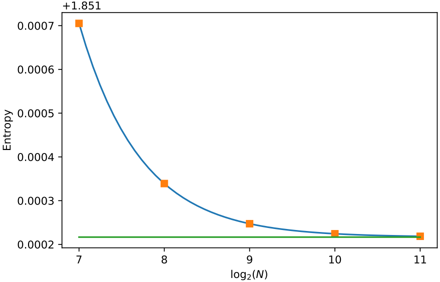

Figure: The entropy of the Angenent torus as computed using 128, 256, 512, 1024, and 2048 points. The values (orange) appear to lie on an exponential curve (blue) converging to 1.8512167 (green).

- The convergence rate suggests that the computed value is within 2×10^{-6} of the true value.
- Later work (Barrett, Deckelnick, Nürnberg, 2020) obtained the same value using different methods.

Vector fields

A naïve approach to vector fields

- Aren't vector fields just tuples of scalars fields?

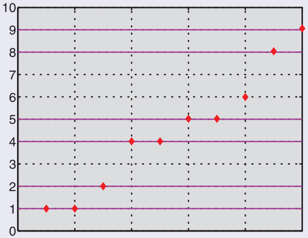

Figure: Numerically computed eigenvalues (red dots) and true eigenvalues (purple lines) for the equation

$$\operatorname{curl}\operatorname{curl} u = \lambda u.$$

Image taken from (Arnold, Falk, Winther, 2010).

- $\lambda = 6???$